Published by :
http://www.ijert.org

International Journal of Engineering Research & Technology (IJERT)
ISSN: 2278-0181
Vol. 4 Issue 09, September-2015

Hydraulic Analysis of Irrigation Canals using HEC-RAS Model: A Case Study of Mwea Irrigation Scheme, Kenya

Imbenzi J. Serede[1*]
[1]National Irrigation Board,
Kenya

Benedict M. Mutua[2]
[2]Department of Agricultural Engineering,
Egerton University, Nakuru, Kenya

James M. Raude[3]
[3]Department of Biomechanical and Environmental Engineering,
Jomo Kenyatta University of Agriculture and Technology,
Juja, Kenya

Abstract:- **Hydraulic simulation models are fundamental tools for understanding the hydraulic flow characteristics of irrigation systems. In this study Hydraulic Analysis of Irrigation Canals Using HEC-RAS Model was conducted in Mwea Irrigation Scheme, Kenya. The HEC-RAS model was tested in terms of error estimation and used to determine canal capacity potential. Thiba main canal reach in Mwea Irrigation Scheme (MIS), approximately 100 Kilometres North East of Nairobi City was selected. MIS being a model scheme in the country, its contribution to food security and growth of the sector is inherent. HEC-RAS model was selected, calibrated and validated using two sets of observed discharges, gate openings and water levels. Statistical and graphical techniques were used for model assessment to establish its performance. The model was finally used to estimate the potential capacity of the main canal reach. The results from this study show that increasing the hydraulic resistance of Link Canal II (LCII) from 0.022 to 0.027 resulted in a decrease in estimated maximum capacity by 10.97%. Whereas for Thiba Main Canal (TMC), increasing the roughness coefficient from 0.015 to 0.016, resulted in a decrease in estimated maximum capacity by 11.61%. Link canal II and TMC therefore were capable of only allowing flows of 9.9 m^3/s and 5.7 m^3/s respectively. This study would be a basis for the scheme management and operators to improve on the operation and management of the irrigation system for effective and efficient water delivery to the farmers.**

Key Words: HEC-RAS; Irrigation; Hydraulic; Canal Reach; Capacity and Discharge

1. INTRODUCTION

Water use and competition among different users has been growing at more than twice the rate of population increase over the last century. For instance, water use for irrigation accounts for approximately 70-80% of the total freshwater available worldwide and irrigation has been ranked as one of the activities that utilize huge amounts of fresh water in many countries. Molden *et al.* (2007) affirms that in the near future, less water will be available for agricultural production due to competition with other sectors. As a result of population growth and rising incomes, worldwide demand for cereals such as rice has been projected to increase by 65% (de Fraiture *et al*., 2007). In addition, Seck *et al*. (2012) projects that global rice consumption will increase to 496 million tonnes by 2020 and further to 555 million tonnes by 2035, and that the aggregate global rice consumption will increase through 2035 due to increased food demand in Africa, Latin America and parts of Asia.

It has further been estimated that the world will need to feed 1.5 to 2 billion extra people by 2025 (Rosegrant *et al.*, 2002). Thus, agricultural sector considered to be the largest water user may face a serious challenge in producing more food with less water (FAO, 2011). Although the expansion on land for agricultural activities has continued to increase over the years, there is still a demand for more food to match the population. This is associated with insufficient water for irrigation to match the increased expansion of agricultural land. However, considerable efforts have been devoted over time to introduce new technologies and policies aimed at increasing efficient water resources management especially for irrigation.

Rice is the third most important food after maize and wheat especially for the urban population in Kenya (Keya, 2013). It is mainly grown by irrigation and water is distributed by surface irrigation systems where water is applied in basins by flooding the paddy fields. To meet the high water requirements, proper water management is inevitable. However, most irrigation schemes in Kenya continue to suffer from chronic water shortages. For instance, in Mwea irrigation scheme (MIS), rotational water application method has been introduced due to constrained water supply. Farmers have thus been divided into three rotational groups on the cropping calendar between the months of August and April (CMC, 2011).

Due to water shortage for irrigation in MIS, it is inevitable that the little available water needs to be utilized in an optimal way. There is need to devise techniques of high Water Use Efficiencies (WUE) in MIS. This can be achieved through several strategies that include; proper

International Journal of Engineering Research & Technology (IJERT)
ISSN: 2278-0181
Vol. 4 Issue 09, September-2015

design of canals, hydraulic structures and proper scheduling for water release to farmers. To achieve this, a total change in operation and maintenance of the systems is required (Maghsoud *et al.*, 2013). In addition, further efforts have been developed to manage the limited available irrigation water. For instance, introduction of New Rice for Africa (NERICA) varieties which thrive in the uplands areas. Further, the use of System of Rice Intensification (SRI) which allows rice paddy to be grown in straight lines at a specified spacing leading to higher yields of rice is also another strategy being used.

Mathematical models have also been used to understand the hydraulic behaviour of complex and large irrigation networks especially for evaluation and improvement of system performance. Some of the common canal flow models in irrigation include; MODIS and DUFLOW (developed by Delft University of Technology), CANAL (developed by Utah State University), CARIMA (Holly and Parrish, 1991), USM (Rodgers and Merkley, 1991), SIC (Cemagref, France), PROFILE (Delft Hydraulic, 1991), FLOP, Mike II (Danish Hydraulic Institute, 1995), DORC (HR Wallingford, 1992), SOBEK (Delft Hydraulic, 1994), MASSCOTE (FAO, 2007), HEC-RAS (developed by the Hydrologic Engineering Center of the United States Army Corps of Engineers) and ODIRMO (Delft University of Technology, 1985).

Irrigation canal simulation studies have been undertaken by Mutua and Malano (2001), Kumar *et al*. (2012), Mishra *et al*. (2001), Shahrokhnia *et al*. (2004), Wahl *et al*. (2011), Maghsoud *et al*. (2013), Hicks and Peacock (2005) and ASCE Task Committee on Irrigation canal system Hydraulic modelling (1993). It is more economical therefore to test and use the present models in comparison with developing new ones (Burt and Styles, 1999).
The main objective of this study was to carry out hydraulic analysis of Thiba main canal reach in Mwea Irrigation Scheme, using HEC-RAS model as a decision support tool for effective operation and management of the irrigation system.

2. MATERIALS AND METHODS

2.1 Description of the Study Area

Mwea Irrigation Scheme (MIS) is located between latitudes 0° 37'S and 0° 45'S and between longitudes 37° 14'E and 37° 26'E. the scheme is within Kirinyaga Kirinyaga County in Kenya and is approximately 100 Kilometres North East of Nairobi as shown in Figure 1. It lies on the Southern outskirts of Mt. Kenya and it covers a gazetted area of 30,350 acres. It is located between 1,100 m and 1,200 m above mean sea level (a.m.s.l).

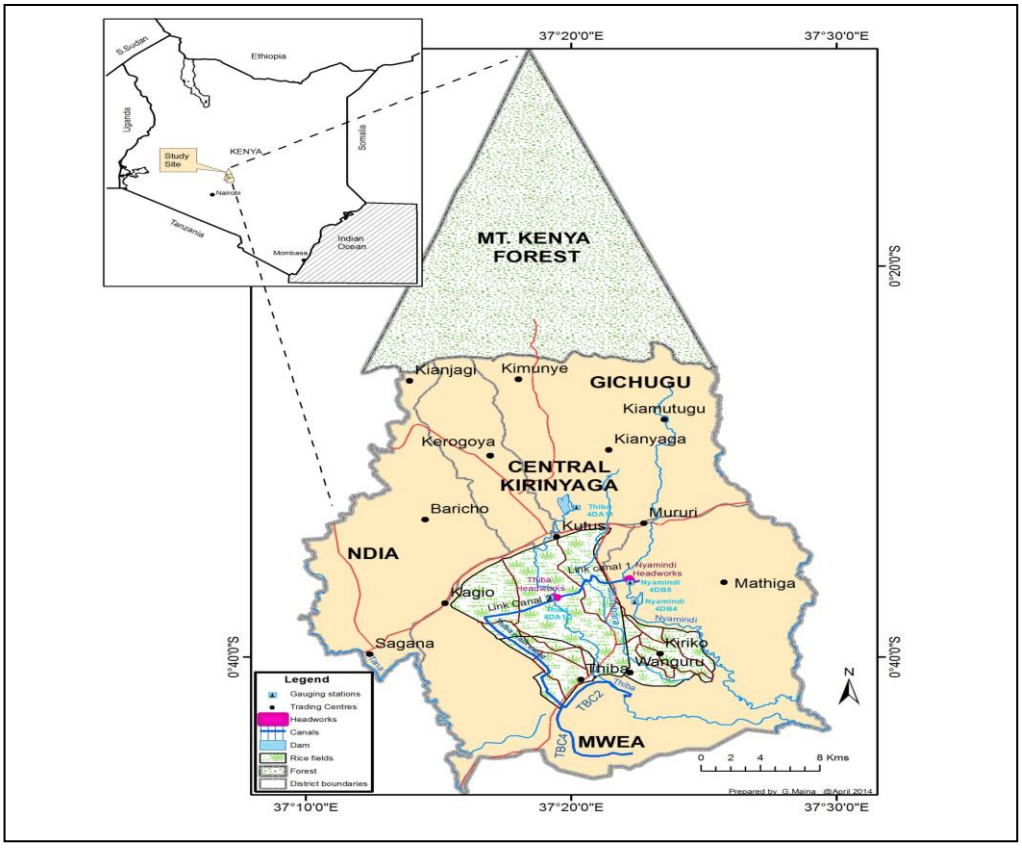

Figure 1: Map of Kenya showing Mwea irrigation Scheme

International Journal of Engineering Research & Technology (IJERT)
ISSN: 2278-0181
Vol. 4 Issue 09, September-2015

MIS is an open gravity irrigation system where paddy mainly Basmati, ITA, IR and BW varieties are grown. There are three head-works that divert water that is used for irrigation in the Scheme from the rivers. The water taken from the Nyamindi head-works flows into the Nyamindi headrace and is then divided into the Nyamindi main canal and the Link canal I. Nyamindi main canal conveys irrigation water to the Nyamindi system. Link canal I is used to convey water from the Nyamindi River to the Thiba River. The Thiba headworks on the other hand abstract water from Thiba River whose flow is increased with water from Link Canal I. This water is conveyed through Link canal II into the Thiba Main Canal. The Rubble weir intake located downstream of Thiba headworks conveys 80% of the water to Tebere Section while 20% is conveyed and used for domestic purposes at MIS staff houses.

The present study focused on Link Canal II reach which is approximately 3.2 km from Thiba intake works and Thiba Main Canal reach, approximately 9.42 km in length. These structures are shown in Figures 2, 3 and 4.

Figure 2: Upstream view of gates at Thiba off-take in MIS

The Link canal II which is shown in Figure 4 has a maximum design capacity of 11.12 m^3/s and the channel beds consist mainly of silt soil and scattered small average cobles. It has an average bed slope of 0.00030 m/m. The second reach, Thiba Main canal (Figure 5) is a stable man-made channel with a 0.00040 m/m gradient that is controlled by a series of drop structures. The concrete lined canal was designed for a maximum flow capacity of about 10.2 m^3/s.

Figure 3: A section of Link canal II

International Journal of Engineering Research & Technology (IJERT)
ISSN: 2278-0181
Vol. 4 Issue 09, September-2015

Figure 4: A section of lined trapezoidal Thiba Main Canal

2.2 Climate

The Scheme area is influenced by seasonal monsoons, with two distinct rainy seasons. The long and short rains occur from April to May and October to November respectively. The scheme receives an average annual rainfall of 940 mm, most of which is received during the long rains as presented in Figure 5.

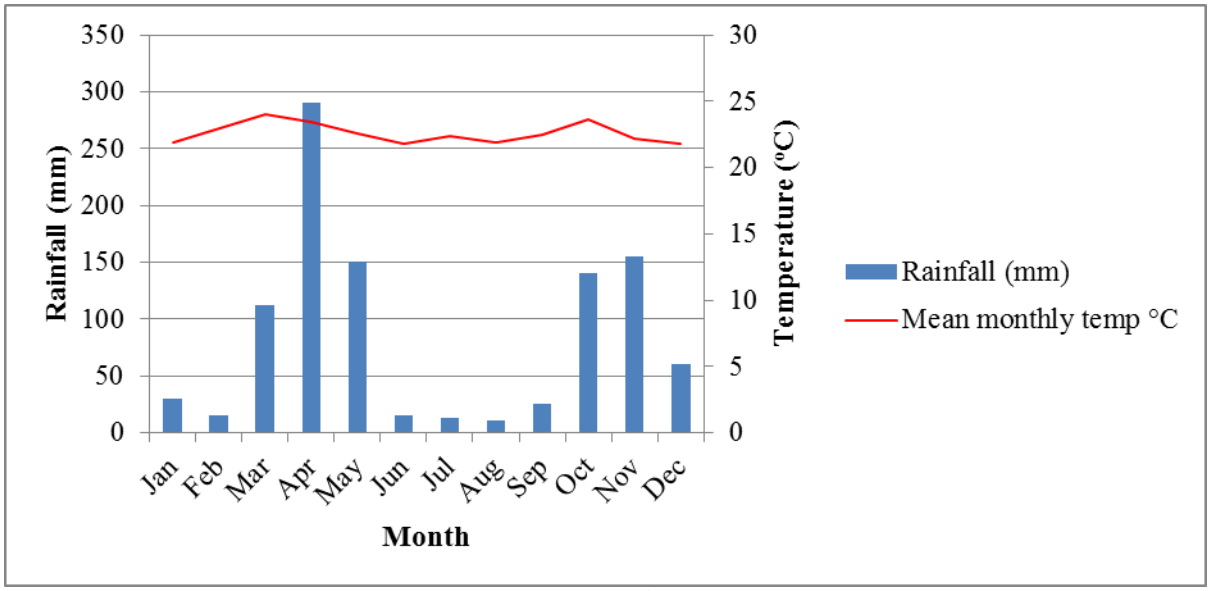

Figure 5: Mean monthly rainfall and temperature

The mean monthly temperature in the scheme area is 22.2°C with a minimum and maximum of 21.8°C and 24.0°C in January and March respectively as presented in Table 1. Generally, the temperatures during the rainy season are higher than those during the dry season (Koei, 2008). The mean monthly evaporation is about 5.8mm/day, with maximum and minimum values of 7.6 mm and 4.2 mm in March and July respectively (Gibb, 2010).

Table 1: Mean monthly rainfall and temperature for MIS (1978-2014)

Month	Jan	Feb	Mar	Apr	May	Jun	Jul	Aug	Sep	Oct	Nov	Dec	Ave.	Max	Min
Rainfall (mm)	30	15	112	290	151	15	13	11	25	140	155	60	84.7	290	11
Mean monthly temp °C	21.9	23.0	24.0	23.4	22.6	21.8	22.4	21.9	22.5	23.6	22.2	21.8	22.2	24.0	21.8

International Journal of Engineering Research & Technology (IJERT)
ISSN: 2278-0181
Vol. 4 Issue 09, September-2015

The cropping pattern in the MIS Scheme was mainly single rice cropping system as presented in Figure 6. Wetland paddy of Group I and II is planted from August to January as the short rain (SR) crop. Wetland paddy of Group III is planted in January and harvested in April. This grouping has been made in order to avoid competition of the limited available irrigation water.

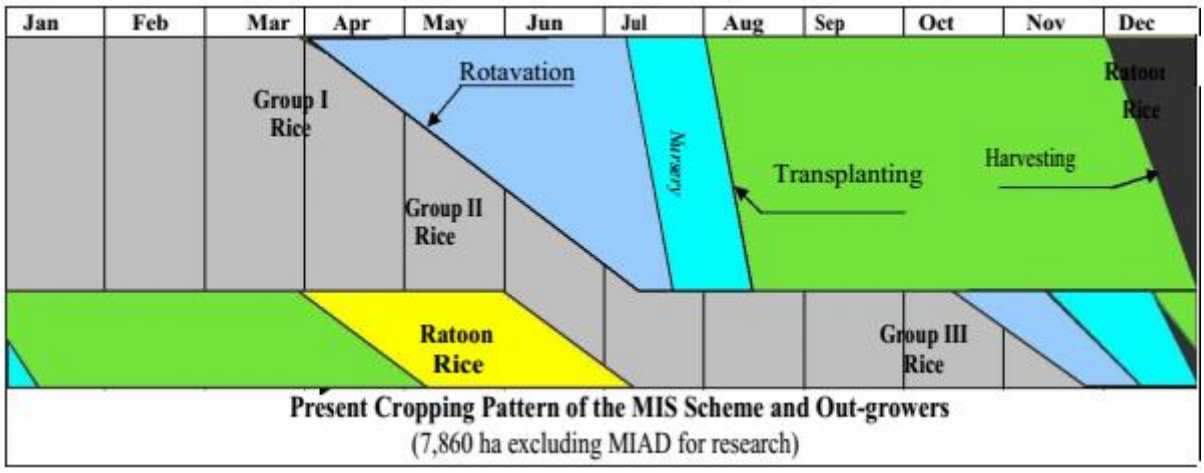

Source: SAPROF (2009)

Figure 6: Present Cropping Pattern of the MIS Scheme and Out-growers

2.3 Vegetation

The original vegetation of the study area is said to have been moist montane forest, scrubland, and cultivated savannah. The upper part of the study area was covered by the Mount Kenya Forest (Gibb, 2010). However, due to the population pressure, some parts of the area have been cleared and replaced with farm crops and eucalyptus forests. The dark-green black wattle trees, scattered eucalyptus trees, cypress and pine trees grow on the hill tops, valley bottoms and along farm boundaries. The swampy areas are dominated with papyrus vegetation. Much of the land in the catchments is under farm crops such as tea, maize, rice, bananas, and horticultural crops.

2.4 Rivers

There are four major rivers in and around Mwea Irrigation Scheme. These rivers are; Tana, Nyamindi, Thiba and Ruamuthambi. There are tributaries branching from the four rivers as shown in Figure 7. These streams are; Murubara, Kituthe, Kiwe, Nyakungu and Kiruara. The main river characteristics and gauging stations in and around the study area are given in Table 2.

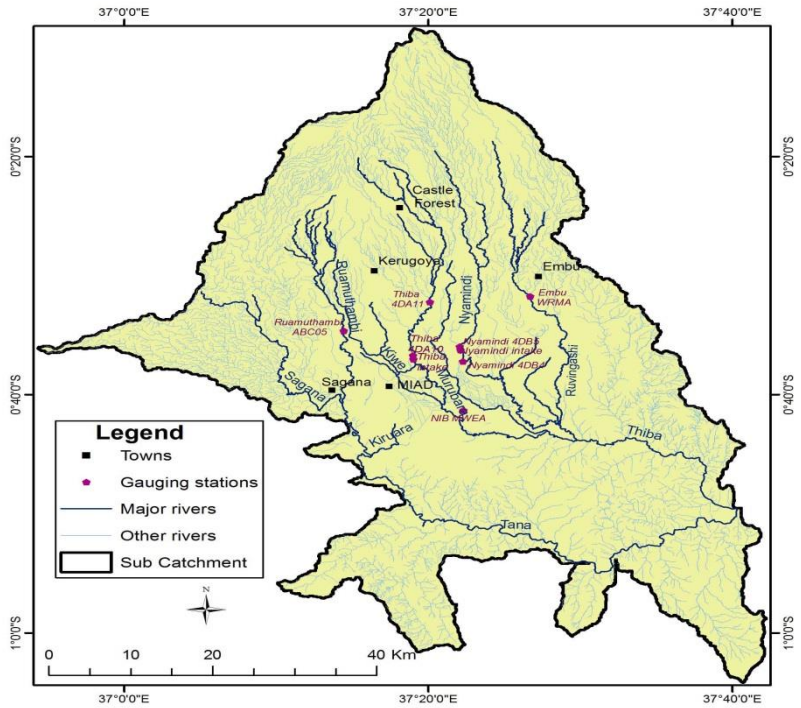

Figure 7: Rivers in and around Mwea Irrigation Scheme

International Journal of Engineering Research & Technology (IJERT)
ISSN: 2278-0181
Vol. 4 Issue 09, September-2015

Table 2: Rivers within the catchment area for Mwea Irrigation Scheme

River name	Gauging stations ID	Catchment area (km^2)	River Length (km)	Mean width of basin (km)	Approximate annual river flow (m^3/s)
Nyamindi	4DB05	283.0	56.9	5.0	6.5
Thiba	4DA10	353.5	47.5	7.4	11.0
Ruamuthambi	4BCO5	86.0	25.3	3.4	2.0
Tana	4BC04	158.0	37.5	4.2	12.5

Source: SAPROF (2009)

2.5 Topography and soils

The area consists of low rolling hills separated by wide flat valleys that have been developed for intensive agriculture. The scheme area generally slopes southward. The western edge of the study area slopes towards Tana River flowing down southward. Soils in the study area consist mainly of Pellic Vertisols and Verto-eutric Nitosols that are both suitable for irrigation farming (Koei, 2008). The black cotton soils are found on the northern high altitude edge of the scheme area. The red soils are mainly coarse-textured with low plasticity and shrinkage rate.

3. HEC-RAS MODEL DESCRIPTION

The Hydrologic Engineering Center's (HEC) River Analysis System (RAS) model was developed by the Hydrologic Engineering Center of the United States Army Corps of Engineers. It is an open source software which can be obtained from the HEC web site: www.hec.uasce.army.mil along with its user manuals. The HEC-RAS model allows one to perform one dimensional (1-D) steady and unsteady flow river hydraulics calculations. It is one of the most commonly used models to calculate water-surface profiles and energy grade lines in 1-D, steady-state, gradually-varied flow analysis. The HEC-RAS model is compatible with and supersedes HEC-2 model (Bookman, 1999). However, in the 1-D, steady-state, gradually-varied flow analysis, the following assumptions were made:

i. There was a dominant velocity is in the flow direction
ii. Hydraulic characteristics of flow remained constant for the time interval under consideration
iii. Streamlines were practically parallel and, therefore, hydrostatic pressure distribution prevails over channel section (Chow, 1959)
iv. Channel slope used for the study is less than 0.1

The model employed a form of the empirical Manning's equation to provide the relationship between the rate of discharge, hydraulic resistance, channel geometry and rate of friction loss. In case of changes in canal prism, energy losses were evaluated using contraction or expansion coefficients multiplied by the change in velocity head.

3.1 Computational methods

The two procedures are the direct and the standard step methods. The direct method is a procedure in which the water depth is known at two locations and the distance between the two locations is considered (Kragh, 2011). Standard step method on the other side applies the hydraulic equations to iteratively calculate water surface profiles and energy grade lines. This method applies the conservation of energy phenomenon in the calculation of water-surface elevations and energy lines along the reach between cross-sections as illustrated in Figure 8.

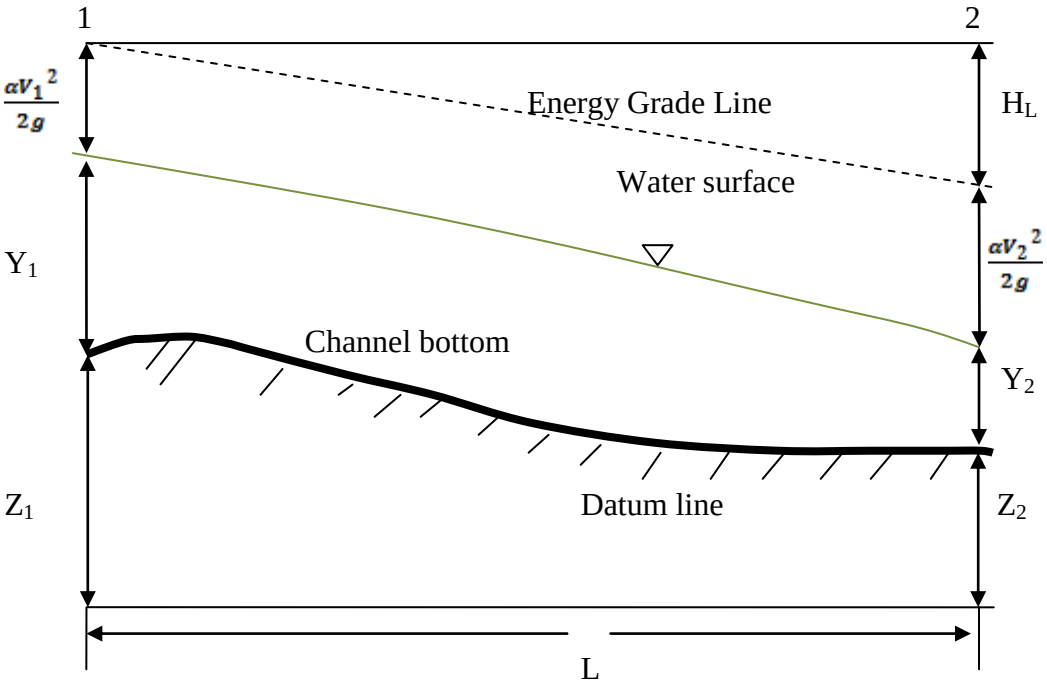

Figure 8: Water surface profiles and energy lines between two points

International Journal of Engineering Research & Technology (IJERT)
ISSN: 2278-0181
Vol. 4 Issue 09, September-2015

3.2 Fundamental functions of the HEC-RAS Model

The fundamental hydraulic equations that govern 1-D, steady-state and gradually-varied flow analysis comprise the continuity, energy and flow resistance equations. In this case, the continuity equation describes discharge as a constant and continuous over a specified period of time. This equation is given as:

$$Q = v_1 A_1 = v_2 A_2 \quad (1)$$

Where,

Q = discharge (m^3/s)

v_1 = average velocity at the downstream (m/s)

v_2 = average velocity at the upstream (m/s)

A_1 = cross-sectional area to the direction of flow at downstream cross-section (m^2)

A_2 = cross-sectional area to the direction of flow at the upstream cross-section (m^2)

The energy equation is used to calculate the total head of water as the summation of the bed elevation, average flow depth and the velocity head at a given cross-section. This equation illustrates the brief principle of water surface study in HEC-RAS model.

$$H = Z + y + \frac{\alpha v^2}{2g} \quad (2)$$

Where,

H = total head of water (m)

α = kinetic energy correlation coefficient

Z = bed elevation at a cross-section (m)

y = flow depth at a cross-section (m)

g = acceleration of gravity (m^2/s)

$\bar{v}$ = average velocity (m/s)

When two channel sections, A and B are taken into consideration with reference to a datum, Equation 2 becomes:

$$Z_A + y_A + \frac{\alpha v^2}{2g} = Z_A + y_A + \frac{\alpha v^2}{2g} + H_L \quad (3)$$

In open channels, the energy equation according to USACE (2008) becomes:

$$(\partial A/\partial t)\,\Delta t = -V_m\,(\partial A/\partial L) - VA_m\,(\partial A/\partial L) \quad (4)$$

Where,

m = subscriptions for the mean values of V and A

L = Channel length (m)

t = Incremental time to be calculated

Energy loss between two cross-sections as illustrated in Figure 8 which comprises friction losses and contraction or expansion losses is given by Equation (5) as:

$$h_e = LS_f + C\left[\frac{\alpha_2 v_2^2}{2g} + \frac{\alpha_1 v_1^2}{2g}\right] \quad (5)$$

Where,

h_e = energy head loss

L = discharge weighted reach length

S_f = representative fraction slope between two stations

C = expansion or Contraction loss coefficient

α_1, α_2 = velocity weighting coefficients

g = gravitational acceleration

v_1, v_2 = average velocities

In canal simulation, channel roughness is one of the sensitive parameters in the development of hydraulic models (Timbadiya *et al.*, 2011). Flow resistance equations used for friction losses estimation are computed with a friction slope from Manning's equation as presented in Equation 6.

$$Q = KS_f^{1/2} \quad (6)$$

Where,

Q = discharge (m^3/s)

K = channel conveyance (m)

S_f = friction slope (m/m)

Conveyance at a cross-section is obtained by Equation 7:

$$K = \frac{\Phi}{n} A R^{2/3} = \frac{\Phi}{n} A\left(\frac{A}{P}\right)^{2/3} \quad (7)$$

Where,

A = cross-sectional area normal to the direction of flow (m^2)

Φ = unit conversion (SI=1.000)

K = channel conveyance (m)

n = roughness coefficient

P= wetted perimeter (m)

R = hydraulic radius (m)

The cross-sectional area and wetted perimeter are a function of channel geometry. If the cross-section is trapezoidal, then the equations used are given as:

$$A = y\,(b + zy) \quad (8)$$

$$P = b + 2y\left(\sqrt{z^2 + 1}\right) \quad (9)$$

Where,

International Journal of Engineering Research & Technology (IJERT)
ISSN: 2278-0181
Vol. 4 Issue 09, September-2015

A = cross-sectional area normal to the direction of flow (m^2)

P = wetted perimeter (m)

y = flow depth at a cross-section (m)

z = side slope of the channel

4. DATA

HEC-RAS model is dependent on a set of data which include canal geometry, channel roughness, energy loss coefficient for hydraulic resistance and the expansion or contraction of flow, discharge and conditions for the flow boundaries of the canal (i.e. top of lining). The geometric data consisted of cross-sectional geometry collected at periodic stations along the study reach. Six cross-sections were uniformly distributed at about 350 m intervals along the Link II Canal. Forty eight sections on the Thiba Main Canal were separated at an interval of 250 m. The sections were surveyed from the top of the left bank to the top of right bank. The cross-sectional data was collected using a dumpy level (Topcon machine X26324 model ATB4). The elevations obtained were based on an assumed, local datum of 1200 m.a.s.l. Illustration of cross-section plots for the Link II Canal and Thiba Main Canal are shown in Figures 9 and 10 respectively. These sections were oriented from left to right in the downstream direction. A positive Cartesian direction was adopted in setting of the start station at the selected cross-section.

The required distribution of cross-sections differ from station to station and depends on site specific features such as longitudinal uniformity of cross-sectional shape, channel linearity, degree of channel meander, longitudinal slope and uniformity of slope throughout the study reach. In this study, cross-section spacing on both canals were determined using Equation 10.

$$D_X = 0.15\,{}^{D}/_{S} \qquad (10)$$

Where,

D_X = cross-section spacing (m)

D = bankful depth (m)

S = bed slope (m/m)

Additional cross-sections were generated by interpolation to aid in model calibration. This was necessitated by factors such as extents of backwater effects due to check structures and changes in canal geometry, drop structures, slope, or changes in canal roughness. At drop structures and falls, cross-sections were located both on the upstream and downstream to accurately define the slope. All elevations were entered in absolute values in the geometry file.

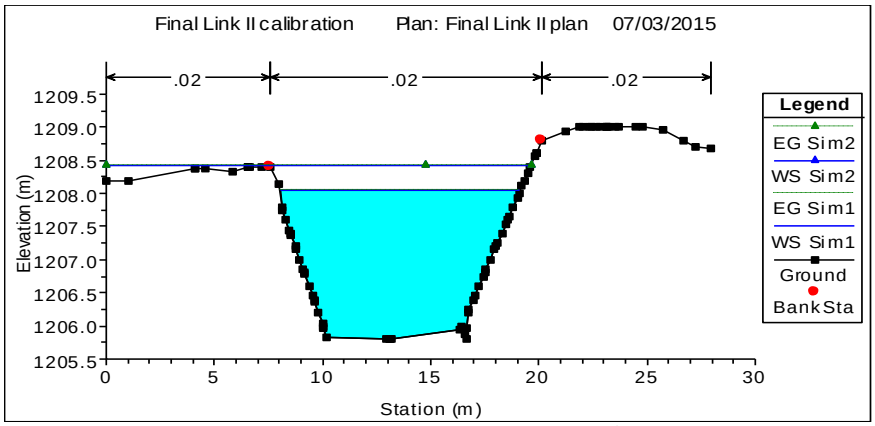

Figure 9: A cross-section showing canal banks and top of lining on LCII

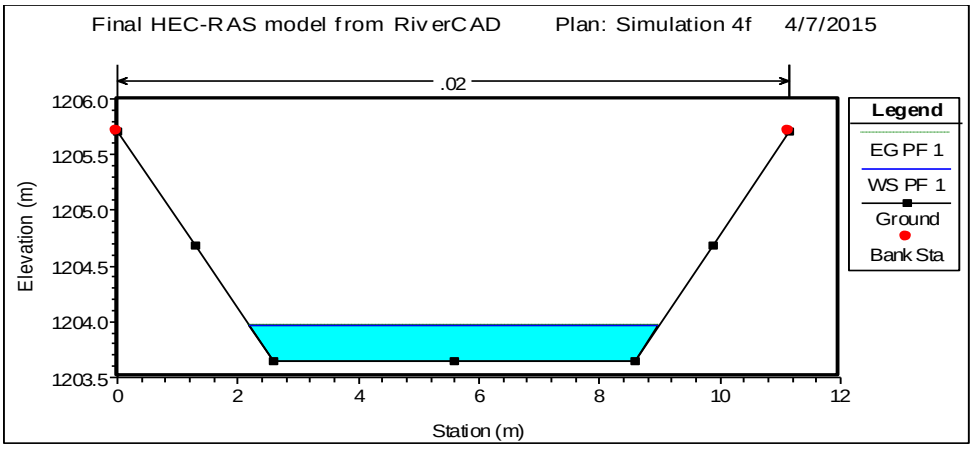

Figure 10: A cross-section showing canal banks and top of lining on TMC

International Journal of Engineering Research & Technology (IJERT)
ISSN: 2278-0181
Vol. 4 Issue 09, September-2015

Actual water surface profiles for each study reach at each flow rate are also surveyed. This is accomplished by surveying the water surface elevation at each cross-section. The profiles are shown in Figure. 11. The water surface elevation at any given section varies across the section due to local turbulence caused by large boulders, etc. The relatively calm water near the banks was used as the measurement location.

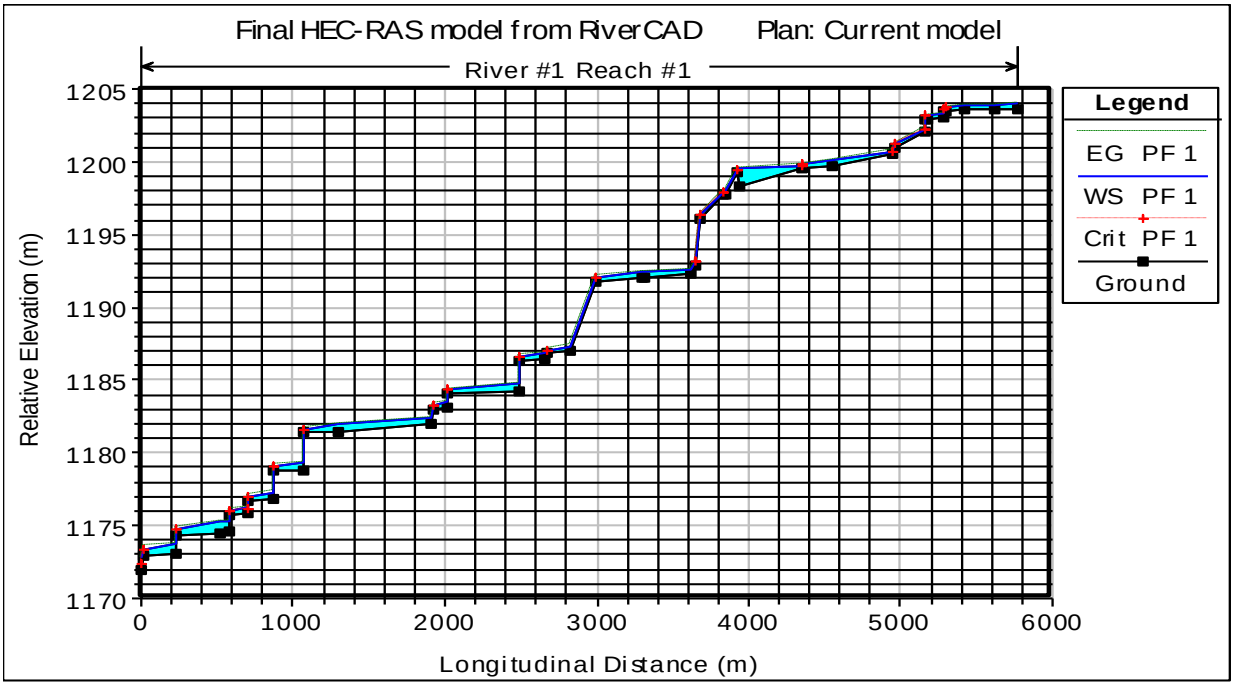

Figure 11: Profile for Thiba Main Canal

5. HEC-RAS MODEL OPERATION, CALIBRATION, SENSITIVITY ANALYSIS AND SIMULATION

5.1 Model operation

With the geometry and flow files established, the HEC-RAS model was executed. This was achieved by selecting Simulate/ Steady Flow Analysis from the project window.

Before running the model, plan definition was created and saved. The plan specified the geometry and flow files to be used in the simulation. This was done by selecting the "File" from the menu bar and then the "New Plan" tab and a plan title was provided as presented in Figure 12.

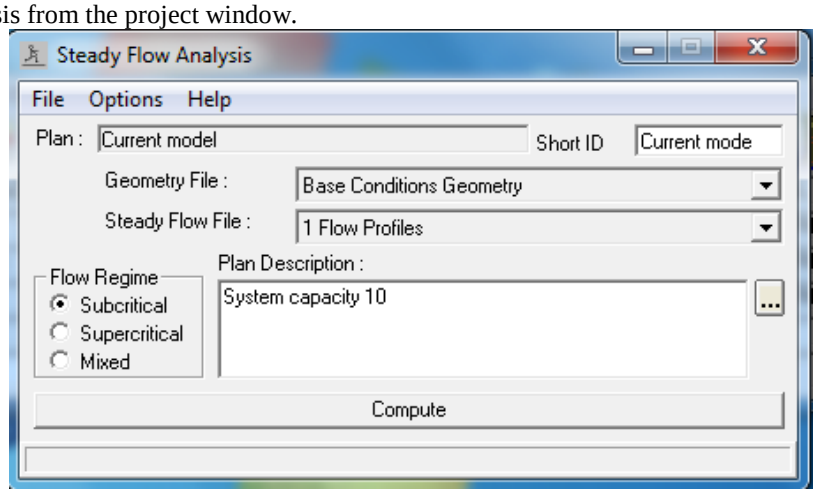

Figure 12: Steady flow analysis window

To execute the model, the flow regime radio button was set to subcritical flow status. To this point all of the HEC-RAS model windows were simply graphical user interfaces used to input data for the model. The computations were performed and results obtained as model outputs in form of graphs and tables. Various runs were done and results recorded.

5. 2 Model calibration

During calibration, Manning's coefficient "n", discharge calibration factors and coefficients were changed iteratively

International Journal of Engineering Research & Technology (IJERT)
ISSN: 2278-0181
Vol. 4 Issue 09, September-2015

until the differences between simulated and observed values of water levels were within the allowable criteria ranges as per the selected statistical criteria. A summary of the procedure followed is given in the conceptual framework in Figure 13. The calibration procedure gave the actual Manning's of the canal which was further optimized.

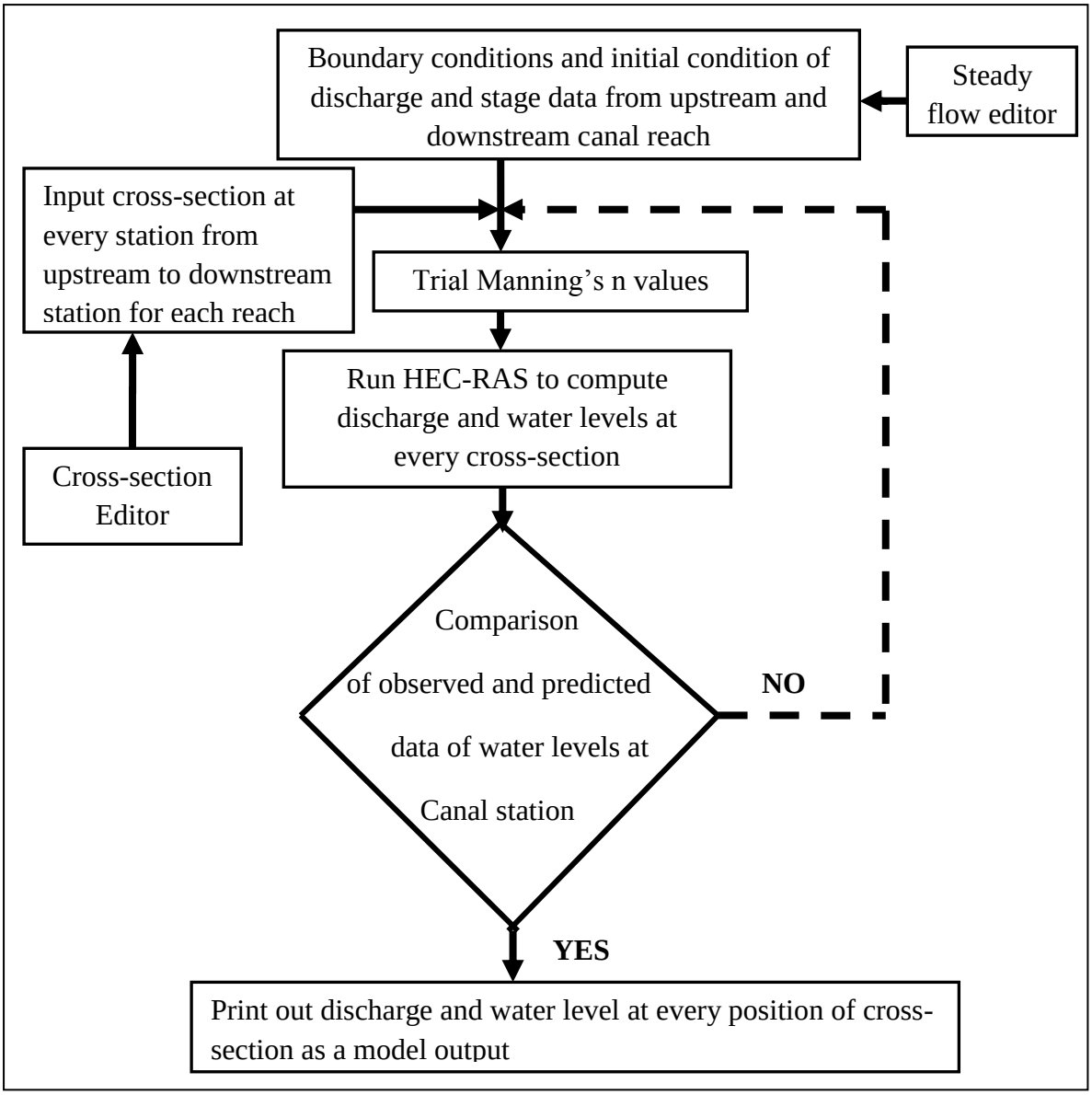

Figure 13: Flow chart of conceptual framework for HEC-RAS Model calibration

Once steady flow simulation was performed, the program output a profile plot including the water elevation that represented the actual water surface profile depth. The modelled energy gradeline was to align parallel to the actual water surface profile. Achievement of this suggested that the canal channel was adequately defined and roughness coefficient appropriately assigned. Four runs were thus carried out for both LCII and TMC.

5.3 Sensitivity analysis

The reliability of the modelling results depends on the capability to accurately estimate these parameters. All parameters selected were confirmed to be within acceptable ranges for the conditions being modelled. A sensitivity analysis was performed on the model to determine the impact of varying discharge, boundary conditions and the manning's 'n' values within the range of values for a given material. For instance, the Manning's value chosen for the concrete lined sections was compared with the recommended values for comparable material in the HEC-RAS Hydraulic Reference Manual, Version 4.1 (USACE, 2001). In addition, the sensitivity analysis was done to determine the impact of varying the Manning's value within the range of values for a given material as per Table 3.

International Journal of Engineering Research & Technology (IJERT)
ISSN: 2278-0181
Vol. 4 Issue 09, September-2015

Table 3: Manning's values used in analysis of earth and lined canals

Type of Channel and description	Minimum	Normal	Maximum
1. Excavated or dredged channels			
a. Earth, straight, and uniform			
1. clean, recently completed	0.016	0.018	0.020
2. clean, after weathering	0.018	0.022	0.025
3. gravel, uniform section, clean	0.022	0.025	0.030
4. with short grass, few weeds	0.022	0.027	0.033
b. Rock cuts			
1. smooth and uniform	0.025	0.035	0.040
2. jagged and irregular	0.035	0.040	0.050
2. Lined or constructed channels			
a. Cement			
1. neat surface	0.010	0.011	0.013
2. mortar	0.011	0.013	0.015
b. Concrete			
1. trowel finish	0.011	0.013	0.015
2. float finish	0.013	0.015	0.016
3.finished, with gravel on bottom	0.015	0.017	0.020
4. unfinished	0.014	0.017	0.020
c. Asphalt			
1. smooth	0.013	0.013	
2. rough	0.016	0.016	

Source: Chow (1959)

5.4 Model validation and optimization

The accuracy of calibrated parameters was tested using the differences between second set of observed data and the new simulated values which validated the model. The suitability of the model was evaluated based on the differences between observed and simulated values by checking the coefficient of determination (R^2) for the observed and simulated values. The expansion and contraction coefficients used in analysing flow test data were 0.3 and 0.1 respectively (Giovannettone, 2008). Inbuilt automatic algorithm within the HEC-RAS model was used for automatic flow optimization through the steady state flow window. The result was checked against values obtained during the calibration process.

6. RESULTS

6.1 Data collection results

Table 4 presents a summary of data collected during the fieldwork. These were used during model simulation, calibration and validation.

Table 4: Summary of data collected during fieldwork

Reach	Distance (m)	Flow (m^3/s)	Water depth (m)	Mean Bed slope (m/m)	Manning's coefficient Min	Normal	Max	Optimized value
Link II	1740	5.80	1.85					
Canal	1490	6.00	2.06					
	900	6.50	2.03					
	640	6.50	2.00	0.00030	0.022	0.027	0.033	0.023
	380	6.50	1.50					
	000	6.50	1.00					
Thiba	2600	0.80	0.32					
Main	2500	0.80	0.35					
Canal	2400	0.90	0.20	0.00258	0.013	0.015	0.016	0.016
	2300	1.20	0.28					
	2200	1.20	0.35					
	2100	1.20	0.35					
	2000	1.20	0.35					
	1900	1.20	0.20					
	1800	1.20	0.28	0.000635	0.013	0.015	0.016	0.016
	1700	1.20	0.20					
	1600	1.20	0.20					
	1500	1.31	0.35					
	1400	1.63	0.20					
	1300	1.63	0.22					
	1200	1.63	0.22					
	1100	1.83	0.22					
	1000	1.83	0.20					
	900	1.90	0.45					
	800	2.00	0.50					
	700	2.00	0.50					
	600	2.00	0.48	0.00050				
	500	2.00	0.70					
	400	3.30	0.40					
	300	3.30	0.40	0.00030				
	250	3.50	0.85					
	000	3.50	1.00					

International Journal of Engineering Research & Technology (IJERT)
ISSN: 2278-0181
Vol. 4 Issue 09, September-2015

From Table 4, the results show average bed slope values of 0.00030 and 0.003895 that were used in simulation of the LCII and TMC respectively. However, for increased accuracy specific slope values of 0.00258, 0.00030, 0.00050 and 0.000635 were used for different cross-sections.

The modelling results vary depending on the number of cross-sections. Typically, it is suggested that cross-sections to be spaced in the order of 90 m to 150 m apart (May *et al.,* 2000). If they are spaced too far apart, the computational algorithm may become unstable and have difficulties balancing the energy between these sections. Cross-section cut lines were drawn covering the extent of the channels in a straight line perpendicular to the flow of the canal. Table 5 presents the number of cross-sections obtained in each reach.

Table 5: Number of cross-sections per reach

Reach	Distance modelled (Km)	Number of cross-sections developed	Number of cross-sections interpolated
LCII	1.74	7	4
TMC	7.17	48	0

6.2 Model parameters

6.2.1 Manning's roughness coefficient

The Manning's roughness coefficient is used to reflect the resistance to flow from the river bottom at each cross-section. The Manning's roughness coefficients for the Thiba main canal reach could not be measured explicitly and was determined through calibration. In this application, roughness coefficients did not vary horizontally across individual cross-sections but were allowed to vary over different reaches specified along the length of the canal reach as presented in Table 6. The main reach was sub-divided into two different calibration reaches in which Manning's roughness was different.

Table 6: Calibrated Manning's 'n' values

Calibration Reach	Distance (m)	Calibrated Manning 'n' Value
Link II Canal	0 to1740	0.023
Thiba Main Canal	0 to 380	0.020
	380 to 7177	0.016

From Table 6, the obtained values were in the range 0.022 – 0.033 for LCII while 0.013 – 0.016 for TMC. The Manning's values obtained by DeVries et al. (2004) after conducting hydraulics of the East Branch of California Aqueduct ranged from 0.0135 to 0.0154 and thus the findings of this research are consistent with latter.

6.2.2 Contraction and expansion coefficients

Contraction and expansion coefficients were set to standard values of 0.1 and 0.3 respectively based on recommendations from HEC-RAS manuals (USACE, 2001). Due to the fact that there are no significant contraction and expansion losses at motorable bridges or check structures in the entire reach, it would be expected that adjusting these coefficients would have little impact on model performance. This was consistent with Giovannettone (2008) findings in the study in St. Clair River in Michigan, where no significant contraction and expansion losses at bridges and other larger obstructions were experienced.

6.2.3 Flow roughness factor

Flow roughness factors were not used in this model since they are features that are useful in calibration of unsteady flow model. This option allows the user to adjust the roughness coefficients with changes in flow. However, calibration and validation results from section 6.4 show that the model did not have difficulty simulating water levels for high and low flow extremes. Also, previous work has shown that calibrated n-values are not affected by flow. These findings further agree with those presented by Giovannettone (2008) in the study carried out in Michigan.

6.3 Sensitivity analysis

A sensitivity analysis was performed on the model parameters, mainly the bed roughness coefficients and model geometry to determine how the simulated flows and water levels were affected by controlled changes. Also, boundary conditions were set to an upstream discharge of 5.54 and 3.65m^3/s for LCII and TMC respectively. Downstream canal stage levels of 1m were applied in all reaches to ensure accuracy of the results due to subcritical flow conditions.

6.3.1 Manning's coefficient

Model runs to test sensitivity of Manning's roughness were performed by increasing and decreasing the roughness coefficients in each calibration reach by eight percent in LCII and six percent in TMC. The results show that an increase in roughness coefficients caused an increase in the water levels simulated for both LCII and TMC, while a decrease in roughness coefficients led to a decrease in water levels simulated for both canals. The largest change in simulated water levels in TMC was 0.45 and 0.12 m in LCII. Generally, the changes occurred when the roughness coefficients were adjusted in TMC reach. This was logical considering that TMC changes affected a larger section of the system

International Journal of Engineering Research & Technology (IJERT)
ISSN: 2278-0181
Vol. 4 Issue 09, September-2015

6.3.2 Cross-section interpolation

This analysis showed that few cross-sections in the LCII geometry could not be accurately used to run the model. The use of few cross-sections yielded errors and warnings which indicated a need for additional cross-sections at canal distance 190, 510, 770 and 1096 m. This caused a change in simulated water level. This result suggested that a sufficient number of cross-sections were necessary in the development of the HEC-RAS geometry to accurately model the canal. Further, it showed that the model was most sensitive in the section surrounding the LCII reach.

6.3.3 Boundary condition adjustment

The boundary conditions of the model were adjusted for two separate cases. In the first simulation, the upstream boundary condition of flow in LCII was adjusted while holding the downstream boundary condition at a known water surface of 0.45 m. This analysis showed that increasing the flow boundary at start of canal to 3.65 m^3/s raised water levels far above the simulated level by 0.40 m.

In the second run, the stage boundaries at LCII and TMC were adjusted while holding the stage boundary at a known water surface at 1m. Figures 14 and 15 shows the trend of increasing roughness coefficient from 0.023 to 0.027 for LCII and decreasing 0.016 to 0.015 for TMC that corresponds to increasing water depth levels for both reaches. The graph shows that under these conditions, the models fitted well to the corresponding measured values.

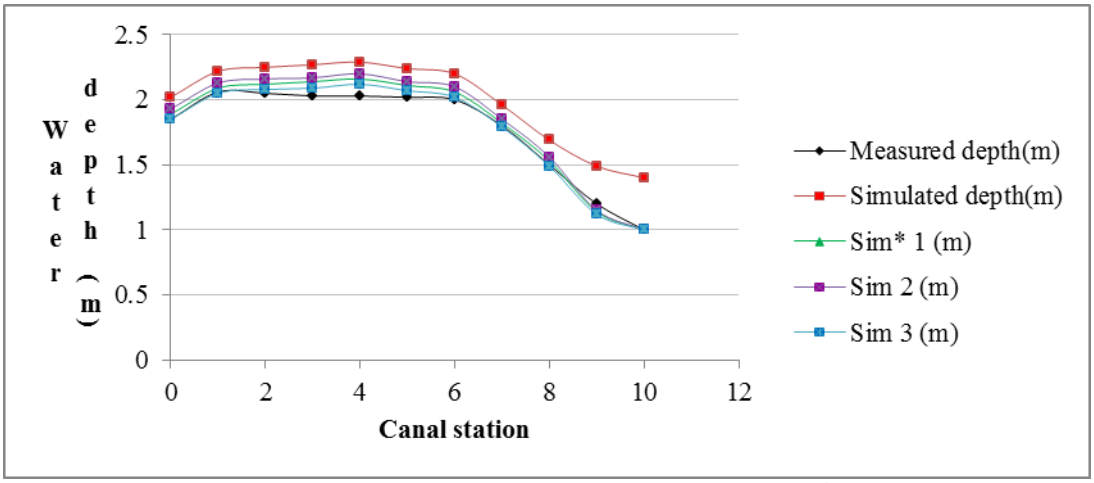

Figure 14: Simulated and measured water depth along the canal stations for LCII

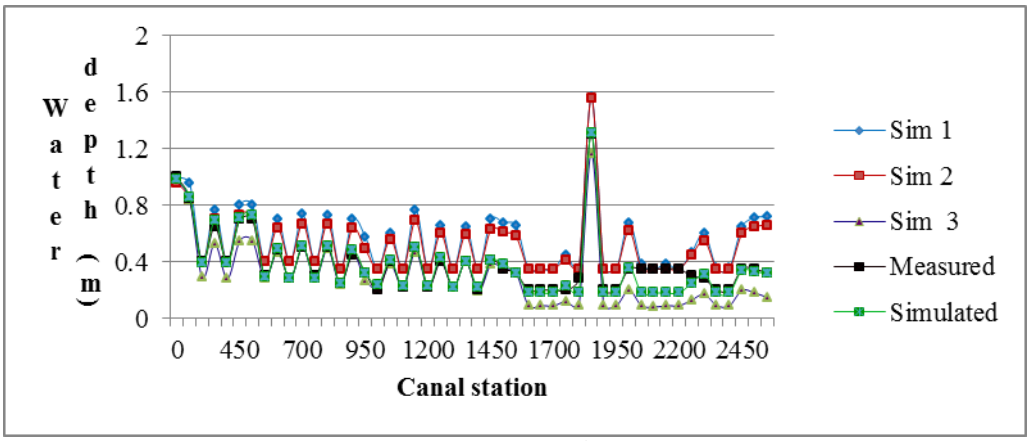

Figure 15: Measured and simulated water depth for TMC along the canal stations

6.4 Model calibration and validation results

The objective of model calibration was to minimize the error between observed and simulated water levels. This was done through the adjustment of Manning's roughness coefficients. The calibration was completed using steady water level and flow boundary conditions. The downstream boundary at LCII and TMC was set at 1 m, and the upstream boundary at LCII was set to a discharge of 5.6 m^3/s while 3.65 m^3/s was set for TMC. The scenario represented approximately average conditions in the Thiba system.

To determine the sensitivity of the model to changes in Manning's roughness coefficient, a range of n-values in a single calibration reach were simulated separately. The HEC-RAS model was executed repeatedly while varying these parameter estimates and the difference between the observed water levels and simulated water levels at canal stations was plotted. Plots of simulated versus measured water levels in each calibration reach are shown in Figures 16 and 17. The Figures show those adjustments of n-values to 0.020 and 0.016 for LCII and TMC respectively. Also, they show that adjustments at certain calibration sections only affect observed water levels at certain canal stations.

International Journal of Engineering Research & Technology (IJERT)
ISSN: 2278-0181
Vol. 4 Issue 09, September-2015

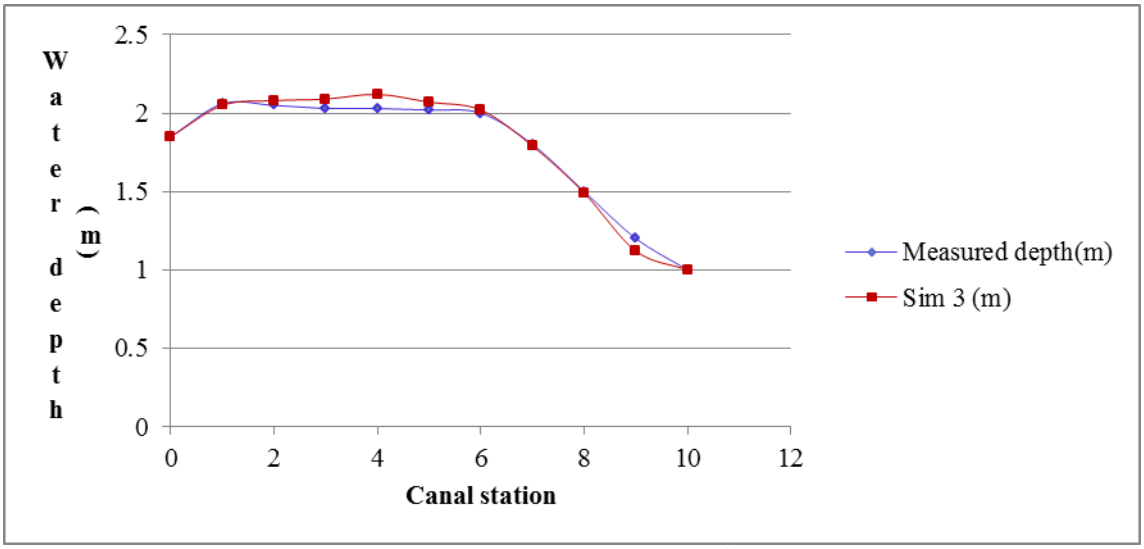

Figure 16: Model behaviour with changes in roughness coefficient to 0.020 in LCII

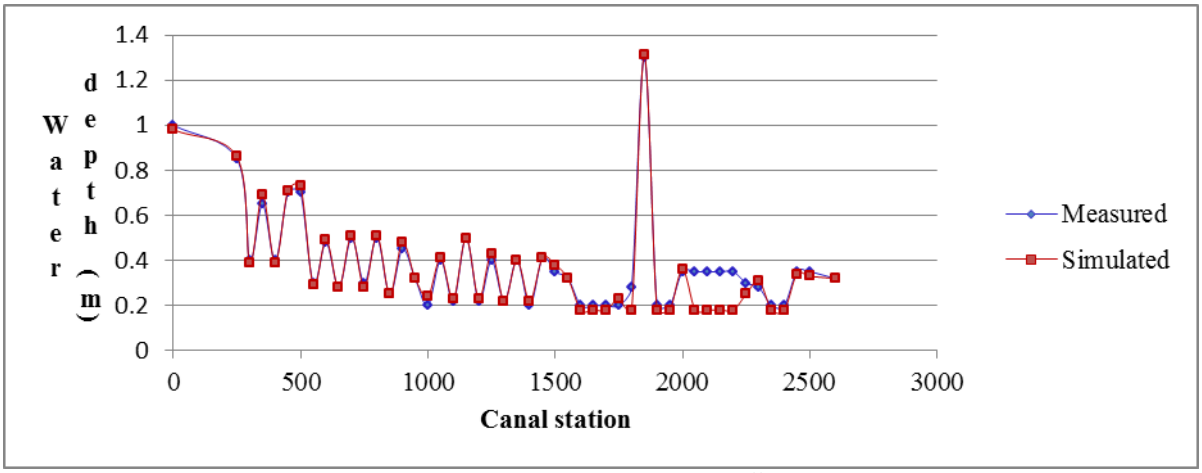

Figure 17: Model behaviour with changes in roughness coefficient to 0.016 in TMC

6.5 Model operation and maintenance procedures

On canal capacity estimation, it was evident that both the two canal reaches could no longer carry the design discharge capacity as per Table 7 and 8 respectively. LCII presented a drop by 10.97% while TMC by 11.61%. For earth canals, in this case LCII, lose their optimal form over time, which causes a reduction in water discharge. Further deformation of the bottom slope in earth canals due to improper dredging and sedimentation changes the canal hydraulic regime and in some cases, reduce canal capacity. With an increase in roughness coefficient, the water level profile is no longer uniform and appears as a gradual variable hence water level changes.

6.6.1 Canal capacities

The estimated canal capacities for the Link Canal II and the Thiba main canal are summarized in Tables 7 and 8.

Table 7: Link Canal II summary of estimated maximum capacities

Reach	Distance (m)	Maximum design flows (m^3/s)	Estimated maximum flows (m^3/s)	Percentage change	(%)
LC II	0 to 1740	11.12	9.9	10.97	

International Journal of Engineering Research & Technology (IJERT)
ISSN: 2278-0181
Vol. 4 Issue 09, September-2015

Table 8: Thiba Main Canal summary of estimated maximum capacities

Reach	Distance (m)	Maximum design flows (m^3/s)	Estimated maximum flows (m^3/s)	Percentage change (%)
TMC	0 to 497	10.20	9.2	9.8
	497 to 1530	6.40	5.8	9.4
	1530 to 3406	6.20	5.5	11.3
	3406 to 4065	6.10	5.3	13.1
	4065 to 4744	5.90	5.1	13.5
	4744 to 5151	5.80	4.9	15.5
	5151 to 6018	5.60	4.9	12.5
	6018 to 7175	5.10	4.7	7.8
	Average		**5.7**	**11.61**

The results show that an increase of hydraulic resistance of Link Canal II from 0.022 to 0.027 and increasing those for TMC from 0.015 to 0.016 resulted in a decrease of maximum canal capacity for the two reaches by 10.97% and 11.61% respectively. These results compare fairly well with those obtained by Derives *et al*. (2014) while carrying out a study in California. Bookman (1999) on the other hand found out that an increase in Manning's 'n' coefficient resulted to 12% and 5% decrease of maximum canal capacity in reach one and two respectively at Beardsley canal for the U.S Bureau of Reclamation. The author attributed the greater effect in reach one to lack of regulating structures in that section.

From Table 6, the reduction of canal capacity in LCII is attributed to absence of regulating structures in the reach, seepage losses and flow within the canal with minimum branching. Table 7 presents an average reduction of discharge to $5.7m^3/s$ for Thiba Main Canal. This reduction in canal capacity is attributed to reduction of canal dimensions during the rehabilitation process. Further, the analysis indicates that the effect caused by a slight change in the roughness coefficient to the canal discharge is substantial. This makes the canal roughness a sensitive parameter.

TMC consists of twenty seven hydraulic drop structures in the main canal path for water transport. This is among the main factors generating flow drop and their effects are sometimes greater than those of roughness coefficients. In addition, the walls of left and right banks have more roughness coefficients than the centre of the earth canal. This issue becomes more severe in modelling of maximum flow rates. This could be the other reason for the impact of 11.61% drop in flow capacity for TMC reach.

6.6.2 Canal bank overflows

It is noted from the results that the integrity of the canal lining in TMC varied from one section to the other. Some sections were in good rehabilitated state while other sections downstream had breaks in the lining. The results show that on LCII, three canal stations 840, 1293 and 1490 were submerged by the design flow rate of 11.12 m^3/s. On TMC, two canal stations at 250 and 1850 were submerged by a design discharge of 6.4 m^3/s. This might have been caused by erosion of the right hand side (RHS) bank on LCII, while changes in canal dimensions during rehabilitation of TMC could be the main cause of bank overflow. Several remedies including canal lining of the LCII could be the long term solution for the canal to carry its design flow capacity.

6.6.3 Distribution plan to units

The modelling results indicate the reduction of canal carrying capacities to an average of $5.7m^3/s$ and $9.9m^3/s$ for TMC and LCII respectively. Managers and operators can therefore make feasible decisions on how water can be distributed to various units based on Table 8. Due to the reduction of canal carrying capacities, distribution plan values must be recalculated or gate opening time increased to achieve the same discharge per 100 ha as indicated.

Table 8: Standard discharge for different water supply to units

Level	Standard discharge (m^3/s/100 Ha)	Period
A	0.18	Flooding season (land preparation)
B	0.12	High ET period
C	0.09	Ponding and transplanting period and during deficit in level B

Source: Abdullahi *et al.* (2009)

6.7 Model evaluation

The model performance results for the LCII canal and Thiba main canal are shown in Figures 18 and 19 respectively. The results in both cases show that the coefficients of determination (R^2) are 0.9927 and 0.9938 for the LCII and Thiba main canal respectively. These results show that the model performed very well.

International Journal of Engineering Research & Technology (IJERT)
ISSN: 2278-0181
Vol. 4 Issue 09, September-2015

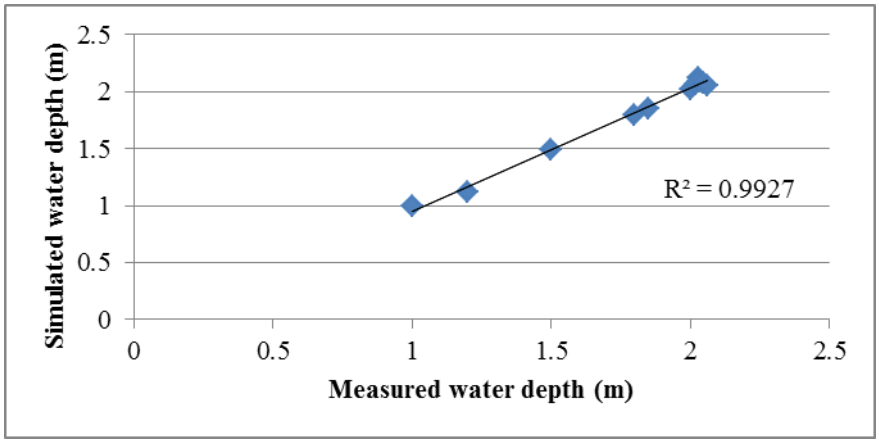

Figure 18: Measured vs simulated water depth for LCII

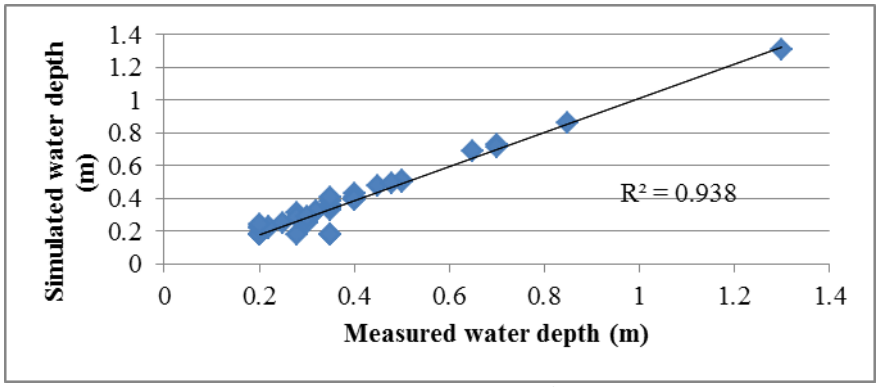

Figure 19: Measured vs simulated water depth for Thiba Main Canal

A plot of coefficient of gain (R^2) revealed that the correlation of the simulated versus measured water depth was relatively high for both sub-reaches. The R^2 value gave information about the goodness of fit of the model. In this regard, the modelled results for LCII and TMC indicated a near perfect goodness of fit of 0.99 and 0.94 respectively which suggested that the modelled simulations were as good as measured water depths. Visual inspection of the scatter plots of simulated versus measured water depths in Figures 18 and 19 show an equally good spread around the line of equal values.

7. CONCLUSIONS AND RECOMMENDATIONS

The HEC-RAS model was calibrated to maximize the coefficient of roughness as the key input parameter. Physical and conceptual parameters were obtained through direct measurement and calibration in the field and derivation using manuals respectively. The coefficient of determination (R^2) values for LCII and TMC were 0.9927 and 0.938 respectively which verified the close agreement between simulated and observed water levels. On canal capacity estimation, both canal reaches could no longer carry the design discharge capacity as LCII and TMC showed a drop in flow capacity by 10.97% and 11.61% respectively.

On formulation of improved operational procedures, the model indicated in each reach, areas of potential bank overflow at specific discharges. Proper dredging by the operators due siltation in the earth canals has been confirmed as a maintenance routine on the system for effective flow. Further, recalculation of water distribution plans and increase of gate opening time for efficient water supply in the system has been suggested.

In this regard, it can be concluded that HEC-RAS is an appropriate model for canal management and operation in MIS. It is further evident that the use of such techniques for the entire MIS canal reach would provide a good tool that could be used to operate different scenarios and its effects on canal system feeding from the main canals. Conversely, care should be taken in selecting, testing and use of the models with respect to the power, utility, accuracy and ease of use as these have an influence on the results. Hence a comprehensive analysis is necessary to facilitate model evaluation in terms of the accuracy of simulated data compared to measured flow rates and constituent value such as water depth.

Based on the results of the HEC-RAS model the following recommendations were made:

i. Calibration and immediate installation of measuring devices directly after the primary off-takes should be of priority by the scheme.
ii. Further research in this model to accurately verify whether the canals were constructed as per the original designs and test model validity and use in other irrigation schemes.

International Journal of Engineering Research & Technology (IJERT)
ISSN: 2278-0181
Vol. 4 Issue 09, September-2015

iii. Lastly, HEC-RAS modelling cannot account for seepage and evaporation losses. Seepage losses cannot be directly accounted for and should be approximated by other techniques. Although the approximations may be sufficient to generally account for the losses, the results may not be satisfactory if seepage losses are of major concern of a study.

REFERENCES

[1] Abdullahi, M., and Tanaka, S. (1995). Mwea Irrigation Scheme Water management manual. *1*: 13.

[2] Bookman, E. (1999). Maricopa Water District Beardsley Canal and associated delivery system hydraulic capacity analysis report, *1(1)*: 1-12.

[3] Chow, V. T. (1959). *Open Channel Flow*. New York, NY: McGraw Hill Publishers.

[4] Corplan Management Consultants (CMC). (2011). *Monitoring and Evaluation Main Report findings,* (Rep. No.03.). Nairobi: CMC Press.

[5] de Fraiture, C., Wichelns, D., Rockström, J., Kemp-Benedict, E., Eriyagama, N., Gordon, L.J., Hanjra, M.A., Hoogeveen, J., Huber-Lee, A., and Karlberg, L., (2007). *Looking ahead to 2050: scenarios of alternative investment approaches*. In: Molden, D. (Ed.), Comprehensive Assessment of Water Management in Agriculture, Water for Food, Water for Life: A Comprehensive Assessment of Water Management in Agriculture. International Water Management Institute, London.

[6] DeVries, J.J., Tod, I.C., and Jensen, M.R. (2004) Study of the Hydraulic performamce of the East Branch, California Aquiduct, J. Amorocho Hydraulics Laboratory, Department of Civil and Environmental Engineering, University of Carlifonia, Davis.

[7] Food and Agriculture Organization (FAO). (2006). *Overview: Rice in Africa a compendium*. Africa Rice 2008. Africa Rice Center, Bouaké.

[8] Food and Agriculture Organization. (FAO). (2011). *The state of the World's land and water resources for food and agriculture. Managing systems at risk*. (Assessment Rep. No.6.). Rome: Publishing Policy and support Branch.

[9] Gibb Africa Limited. (2010). *Mwea Irrigation Development Project Design review main report. 1*: 36-37.

[10] Giovannettone, J. (2008). *Preparation of the 1-D St. Clair River HEC-RAS Model in order to study changes in River conveyance and morphology. 1*: *4-43*.

[11] Hicks, F., and Peacock, T. (2005). Suitability of HEC-RAS for flood forecasting. *Canadian water resources journal*, *30* (2): 159-174.

[12] Keya, O. S. (2013). *More rice Less water*. (3rd ed.). Nairobi, Kenya: East African publishers.

[13] Koei, N. (2008). *Mwea Irrigation Development Project Design main report. 2*: 28.

[14] Kragh, E. M. (2011). *Flood capacity improvement of San Jose Creek Channel using HEC-RAS*. San Jose Creek, California.

[15] Kumar, P.P., Sankhua, R.N., and Roy, G.P. (2012). Calibration of channel roughness for Mahanadi River (India), using HEC-RAS Model. *Journal of water resources and protection*, *4*: 847-850.

[16] Maghsoud, A., Alireza, P., and Majid, R. (2013). Study and simulation of Hydraulic and structural changes of changing of section from soil to concrete. *Middle East Journal of Scientific research.* IDOSI publications.

[17] May, D.R., Lopez, A., and Brown, L. (2000). *Validation of the hydraulic-open channel flow model HEC-RAS with observed data.* Available from www.hec.usace.army. (Accessed 20th May, 2015).

[18] Mishra, A., Ghorai, A.K., and Singh, S. R. (1997). Effects of the dike height on water, soil and nutrient conservation and rice yield. *ICID Journal 48* (3).

[19] Molden, D. (2007). *Water for Food, Water for Life: A Comprehensive Assessment of Water Management in Agriculture.* Earthscan and International Water Management Institute. London and Colombo.

[20] Mutua, B.M., and Malano, H.M. (2001). Analysis of manual and centralized supervisory control operations to improve level of service: a case study of Pyramid Hill No. 1 Channel, Victoria, Australia. *Irrigation and drainage journal*, *1*(3): 1-19.

[21] Rosegrant, M. W., Cai, X., and S. A. Cline. (2002). *World Water and Food to 2025: Dealing with Scarcity.* International Food Policy Research Institute. Washington DC.

[22] SAPROF (2009). Mwea Irrigation Scheme Special Assistance for Project Formulation report Safeguards on ESIA and RAP.

[23] Seck, P.A., Diagne, A., Mohanty, S., and Wopereis, M.S. (2012). Crops that feed the world 7: rice. *Journal of Food Security*, *4*: 7-24.

[24] Shahrokhnia, M.A., Javan, M., and Keshavarzi, A.R. (2008). Application of HEC-RAS and MIKE-11 models for flow simulations in irrigation canals. *Journal of Agricultural Engineering, 23*,(4): 4-11.

[25] Timbadiya, P. V., Patel, P. L., and Porey, R.D. (2011). Calibration of HEC-RAS model prediction of flood for lower Tapi River, India. *Journal of water resources and protection, 3*, (6): 5-11.

[26] U.S. Army Corps of Engineers. (2001). HEC-RAS: User's and hydraulic reference manuals.

[27] Wahl, T. L., and Lentz, D. J. (2011). *Physical hydraulic modelling of canal breaches*. Hydraulic Laboratory Report HL-2011-09, U.S. Dept. of the Interior, Bureau of Reclamation, Denver, Colorado, 56.

[28] Wahl, T.L. (2004). *Issues and problems with calibration of Canal Gates*. World water and Environmental resources Congress, Salt Lake City, UT, June 27-July 1, 2004 Environmental and Water Resources Institute of the American Society of Civil Engineers.